

CLASSIFICATION OF COUPLED LINEAR MOTORS BY USING A DEVELOPMENT METHODOLOGY

MATTHIAS REHM, JOHANNES QUELLMALZ, HOLGER SCHLEGEL AND REIMUND NEUGEBAUER

Technische Universität Chemnitz
Professorship for Machine Tools and Forming Technology
Institute for Machine Tools and Production Processes
Chemnitz, Germany

DOI: 10.17973/MMSJ.2015_06_201521

e-mail: matthias.rehm@mb.tu-chemnitz.de

This paper presents a holistic development methodology with functional correlations between the mechanical and electrical parameters which is used for an optimization of feed drive systems with more than one drive. Within this process-oriented development methodology, the adaption of the controller is of central importance. Using the example of a new designed linear drive characterized by two mechanically coupled and opposite driving linear motors the potential of various control structures for coupled drives are going to be investigated. Next to the improvements of the drive arrangement, tuning methods for the different structures as well as experimental and simulation results are discussed.

KEYWORDS

design, development methodology, feed axes, electromechanical drives, coupled linear drive

1. INTRODUCTION

Feed drive systems are distributed in a large field of production systems. Depending on their range of tasks different electrical and mechanical structures are established. Typically a distinction is made between feed drive systems with gears such as ball screw or rack and pinion drives and direct linear drives, short linear motors [Altintas 2011]. Feed drive systems with gears are used as a standard application due to their wide power range and cost-efficient structure and implementation. However, those feed drives systems are dynamically limited caused by the mechanical structure representing a multi-mass system with several eigenfrequencies. At this point, linear motors show much better dynamical behaviors since its mechanical structure has no elastic coupling elements.

2. INITIAL SITUATION

As a standard method, electromechanical feed axes are designed according to the stationary and dynamic forces and moments. All

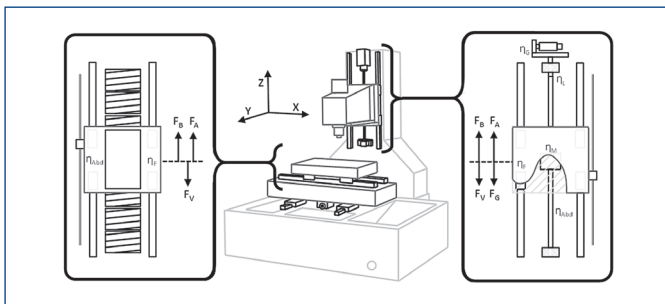


Figure 1. 5-axis machining center with typical feed drives (left – ball screw; right – linear motor)

considerations are based on the equilibrium of forces on the considered feed axis. Fig. 1 is representing a typical standard production machine, a 5-axis machining center, with a vertical Z-axis with a ball screw drive (right) and a horizontal X-axis with a linear motor (left).

During the machining process, both axes are subjected on the one hand with stationary forces such as the machining forces F_B , the losses F_V and the weight F_G , on the other with dynamic forces of the acceleration force F_A . In terms of a uniform nomenclature all of the following considerations are based on the forces. The equivalent torques $M = i_{kl} \cdot F$ for feed axes with gear conversion result on the corresponding gear constant i_{kl} .

The constants for a ball screw i_{BS} and a rack-and-pinion i_{RP} are given to:

$$i_{BS} = \frac{p_{Sc}}{2 \cdot \pi \cdot i_G} \quad \text{and} \quad i_{RP} = \frac{r_{Pi}}{i_G} \quad (1), (2)$$

with:

p_{Sc} = pitch of the screw

r_{Pi} = radius of the pinion

i_G = gear ratio

The sum of the stationary forces can be achieved by analyzing the specific feed drive system in relation to the lossy components. For this reason Fig. 2 gives an overview about all common feed axis mechanisms. In the upper row, all single axis mechanisms can be found starting on the left with a ball screw drive (A), a belt drive (B) and a rack-and-pinion drive (C) in the middle. Next to these drives with a gear unit, the single axis mechanisms without any gear can be found.

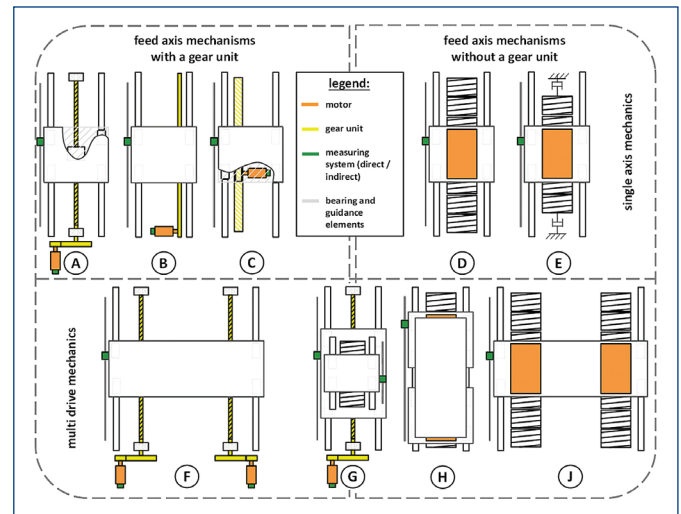


Figure 2. Overview about all common single and multi feed drive mechanism

This group contains a classical linear motor (D) and an impulse decoupled linear motor (E) [Denkena 2009]. Beside the single axis mechanisms, within the industrial field of feed drives, multi drive mechanisms, shown in the lower row in Fig. 2, can be found. They are used due to higher forces and a symmetrical force distribution. The most left mechanism is a dual ball screw drive in gantry embodiment (F) moving one slide. The piggyback mechanism (G) with a ball screw drive and a linear motor represents a hybrid system. Linear motors shows high dynamics but are limited to their maximum force that correlates to the geometrical parameter of the drives. Based on this, multi motor structures are realized such as the mechanism with two motors on one secondary part (H) or the already mentioned gantry mechanism (J). In consequence, both multi linear motor mechanics lead to higher excitations of the machine structure.

According to the feed axis mechanism the number of lossy components such as gears, bearings or linear guiding varies [Weidauer 2011].

Generally speaking, direct drives have less lossy parts and a high dynamic due to missing weak gear units. The sum of the stationary forces, called load force, depends on the mechanism and is calculated for a feed drive with gear unit $F_{L_{wG}}$ to the formula

$$F_{L_{wG}} = \frac{i_{kl}}{\eta_{kl}} \cdot [F_{Ma} + F_{G_{const}} + \mu_G (m_{sum} \cdot g \cdot \cos \alpha + F_{Ma_G}) + F_{cov} + \frac{\pi \cdot \mu_{Bear} \cdot \eta_M \cdot d_{b_{Sc}} \cdot F_{ax_{Sc}}}{h_{Sc}} + m_{sum} \cdot g \cdot \sin \alpha] \quad (3)$$

The load force of a drive mechanism without any gears $F_{L_{LD}}$ can be calculated by

$$F_{L_{LD}} = F_{Ma} + F_{G_{const}} + \mu_G (m_{sum} \cdot g \cdot \cos \alpha + F_{Ma_G} + F_{Att}) + F_{cov} + m_{sum} \cdot g \cdot \sin \alpha \quad (4)$$

All symbols and meanings of the parameter in (3) and (4) are listed in the table beside. For the calculation of the load forces, all parameters have to be taken into account according to the forms and geometry of the feed drive.

Symbol	Meaning of the parameter
$d_{b_{Sc}}$	mean bearing diameter of the screw
g	gravity
h_{Sc}	screw pitch
m_{sum}	maximum moved mass
F_{att}	attraction force (only for mechanism without a gear)
$F_{ax_{Sp}}$	axial force of the screw
F_{cov}	friction force of the cover
$F_{G_{const}}$	constant friction force of the linear guiding
F_{Ma}	machining force
F_{Ma_G}	perpendicular vectorial part of the machining force
α	tilt angle of the feed drive
η_M	efficiency factor of the ball nut screw
η_{kl}	efficiency factor of the gear
μ_G	friction factor of the linear guiding
μ_{Bear}	friction factor of the rolling bearing

Table 1. Symbols and meanings of the parameter

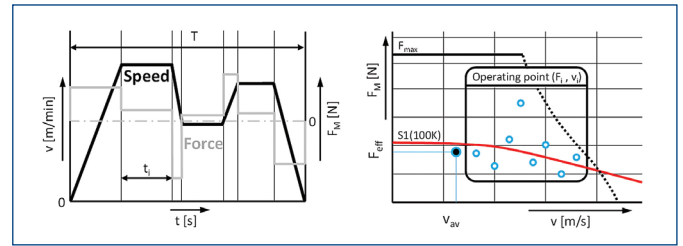


Figure 3. Free load cycle (left) and the resulting force/velocity diagram (right)

In this context, the technical literature [Chen 2005, Hamann 2006, Schroeder 2001 and Zirn 2008] and datasheets of the manufacturers should be consulted.

Next to the stationary forces, the dynamic forces and thermal stresses are going to be determined. Both depend largely on the motion function and the nominal operating mode [Bruckl 1999]. Normally, a free load cycle as shown in Fig. 3 (left) is given. Out of this, several operating points (Fig. 3, right) are the result. The average value of the velocity and the effective value of the force need to be below the S1-line. Otherwise, thermal problems might occur. Within the design process, some basic rules have been established. The acceleration force should be at least twice as much as the standstill force and the ratio between the motor mass and the moved mass should be with 1 to 3.

The whole design process can be seen in Fig. 4 on the left side. It is characterized by an iterative approach at the different levels. First the determination of the stationary and dynamic forces with the comparison between the run-up time and the acceleration time as the first loop condition. Next, the average forces (as explained in Fig. 3) are determined. In case of any violations, the drive or the mechanical parts (inertia) have to be changed manually. After a proper drive is found, the drive electronics have to be chosen. At the end of the iterative design process, a suitable feed drive is found.

3. GOAL AND APPROACH

The present state of the art design process does not take any interaction between drives into account nor is it an automated process. Furthermore, the controller structure and design, both important parts within the design process, are uncovered. For this reason, all current feed

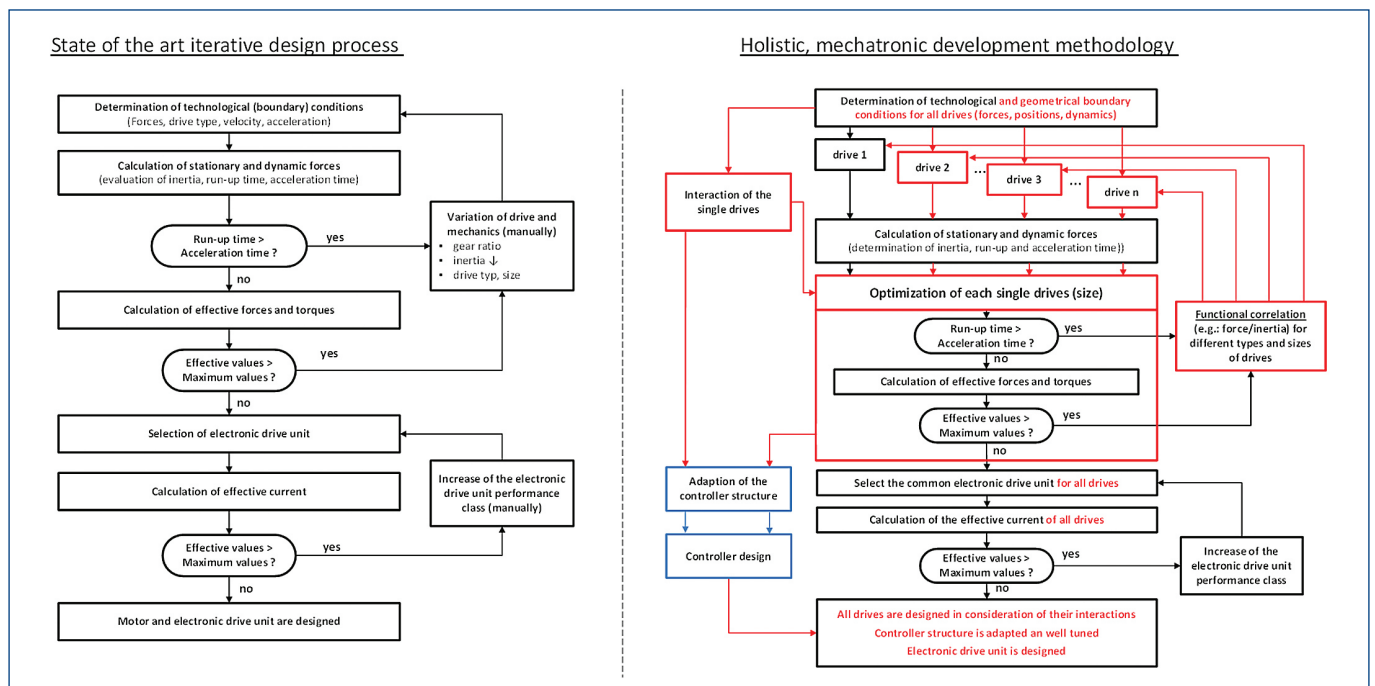


Figure 4. Iterative design process (left) and process-oriented development methodology (right)

drives and their controllers were design based on a large knowledge base. On the one hand, this allows only limited comparability between different feed drives, on the other hand the controller structure is not adopted to the special boundary conditions of multi drive mechanisms, so called coupled drives. As mentioned in Chapter II about Fig. 2, linear motors offer, compared to feed drives with gears, much higher dynamics but are limited to their maximum force [IEC 6034-1:2004]. Negative aspects of the higher dynamics are the reaction forces into the machine structure causing undesired excitations. By using a multi motor mechanism, the maximum forces but also the reaction forces are increased. Decoupling structures like the impulse decoupling of the secondary part leads to reduced excitations by are also limiting the dynamics. Within this paper a novel coupling mechanism of two linear motors is going to be presented. This arrangement, shown in Fig. 5, improves the static and dynamic properties by force distribution which leads to an impulse-free feedback system. To exploit the gained dynamics various control structures for coupled drives need to be adopted, designed and investigated.

4. NEW DESIGN APPROACH AND MECHATRONIC METHODOLOGY

As an advancement of the state of the art iterative design process, a holistic mechatronic development methodology [Rehm 2015], shown in Fig. 4 on the right side, was used to find and evaluate the new coupling mechanism. Red shown are the additional and/or changed steps during the design process. Within the methodology, more than one drive can be designed and their interactions are taken into account. By optimizing each drive based on functional correlations, an optimal solution, that is going to be presented, could be found. Beside the mechanical structure, the focus of this paper deals with the controller adaption and design, shown blue in Fig. 4. This novel approach represents a force decoupled feed drive system, as schematically illustrated in Fig. 5 (left), characterized by two mechanically coupled linear motors that move in opposite directions relative to each other.

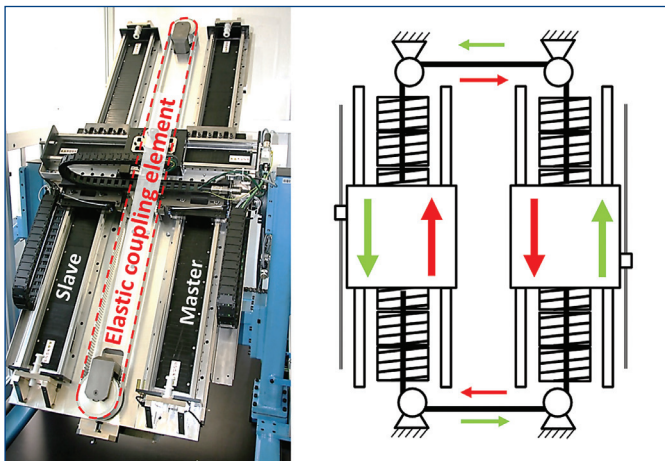


Figure 5. Realized test rig (left) and fundamental functionality (right)

Preference of this structure is the power distribution between the both drives by coupling them with a flexible belt. By this, the dynamics can be improved due to the compensation of the reaction forces. Furthermore, this drive structure allows the storage of energy within the linking element that can be used to cover power peaks. For achieving the optimal results out of the arrangement, effective control strategies need to be examined. Therefore, the following section exposes selected control structures for coupled drives and their parameterizations.

5. CONTROLLER STRUCTURES

Basically, all following control structures and algorithms are intended to be realized on an industrial servo control. The concept of an industrial

servo control has been established successfully caused by its good possibilities for parameterization and dynamic characteristics. Since this control is restricted in its flexibility, several advanced control concepts were investigated. Regardless of the specific control algorithm, a well parameterized control cascade is the basis. Thus, the structure with their parameters is going to be presented first.

The current control loop, which is the innermost control loop of a servo control, is realized by a PI-current controller with a set point filter. Its dynamic behavior can be reduced to a transfer function with a first order element plus dead time like:

$$G_{sub,i}(s) = \frac{e^{-T_{dead,i}} \cdot s}{T_{sub,i} \cdot s} + 1 \quad (5)$$

Both the dead time $T_{dead,i}$ and the time consistent of the current control loop $T_{sub,i}$ rely on the electrical motor, the power electronics and the control system. The controller is tuned to the optimum amount as in [Schroeder2001]. Overlaid to the current controller, the PI-speed controller has to be tuned. Based on the open speed loop $G_{o,v}(s)$, the gain K_p and the integral time $T_{N,v}$ are adjusted by tuning rules like symmetrical optimum, Shinsky I or Samal.

$$G_{o,v}(s) = K_p \cdot \left(\frac{T_{N,v} \cdot s + 1}{T_{N,v} \cdot s} \right) \cdot \frac{1}{J_{sum}} \cdot \frac{e^{-T_{dead,i}} \cdot s}{T_{sum,v} \cdot s} \quad (6)$$

By using the total inertia J_{sum} as well as the substituted time of the speed control loop $T_{sum,v}$ the parameters for the velocity controller can be found in Table 2. The position controller with its amplifier gain K_V the feed forward control K_{pc} and the symmetry filter T_{vic} is the outer control loop. Its closed loop is represented by:

$$G_{c,x}(s) = \frac{K_V}{T_{sub,v} \cdot s^2 + s + K_V} \quad (7)$$

Based on the equivalent time constant $T_{sub,v}$ of the underlaid velocity control loop the amplifier gain can be estimated by the following equation:

$$K_V = \frac{1}{T_{sub,v} \cdot A} [1/s] \quad (8)$$

Rule	Parameterization	
	K_p [Ns/m]	$T_{N,v}$ [ms]
Symmetrical Optimum	$\frac{0.5 \cdot J_{sum}}{T_{sumv} + T_{deadi}}$	$4 \cdot (T_{sumv} + T_{deadi})$
Shinsky I	$\frac{0.556 \cdot J_{sum}}{T_{sumv} + T_{deadi}}$	$3.7 \cdot (T_{sumv} + T_{deadi})$
Samal	$\frac{\pi}{4} \cdot \frac{J_{sum}}{T_{sumv} + T_{deadi}}$	$3.3 \cdot (T_{sumv} + T_{deadi})$

Table 2. Tuning rules for PI velocity controller [ODwyer2006]

Within eq. (8), A represents a tuning parameter that influences the damping of the closed position loop. It can be chosen between an aggressive ($A=2$) or an aperiodic ($A=4$) behavior. By choosing the feed forward control $K_{pc} = 0.8$ a stable and dynamic behavior of the position loop can be achieved. The selection of the filter time constant T_{vic} depends the already introduced equivalent time constant $T_{sub,v}$ of the underlaid velocity control loop and the communication time T_{com} of the applied controller solution, which is typically between two up to three cycle times. By this, the filter time constant can be estimated by the following correlation:

$$T_{vic} = T_{sub,v} + T_{com} [ms] \quad (9)$$

Following the parameterization of a servo control, the investigated control structures are taken into account. A lot of research work has been done on the Parallel-Synchronous-Control (PC), Master-Slave-Control (MSC), Cross-Coupled Control (CCC) and Relative Stiffness Control (RSC). As standard industry applications, the tuning rules for PC and MSC can be found in literature [Nakamura2004]. The following part considers more deeply the advanced control structures of RSC and CCC.

RSC, the first investigated advanced control structure for coupled drives, is shown in Figure 6. It is based on a position controlled master drive with a velocity controlled slave drive. For the minimization of velocity differences between both drives an additional synchronous controller $S(s)$ is integrated. Based on velocity differences additional currents are computed and signed connected to the master and the slave drive.

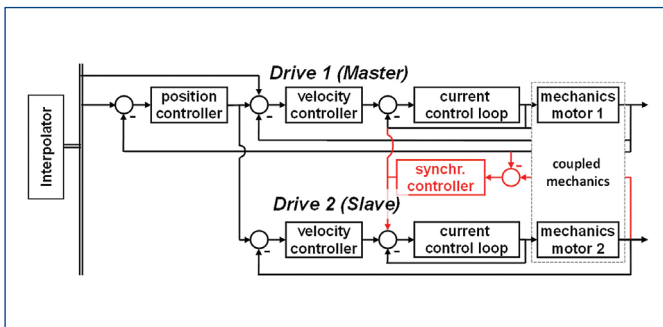


Figure 6. Structure of the Relative Stiffness Control

The task of the synchronous controller is the minimization of the synchronous error, which can be depicted as:

$$E(s) = \frac{E_0(s)}{1 + S(s) \cdot G_{sum}(s)} \quad (10)$$

Within eq. (10), $E_0(s)$ represents the synchronous error without $S(s)$. The transfer function $G_{sum}(s)$ represents the speed drive controlled coupled mechanics:

$$G_{sum}(s) = G_{MM}(s) - G_{SM}(s) + G_{SS}(s) - G_{MS}(s) \quad (11)$$

with the different transfer functions (motor side $G_{MM}(s)$ and $G_{SS}(s)$; load side $G_{SM}(s)$ and $G_{MS}(s)$). By selecting a limiting frequency ω_s , the control objective can be described by:

$$\max\left(\frac{1}{1 + S(s) \cdot G_{sum}(s)}\right) \leq 1, \omega \leq \omega_s \quad (12)$$

Similarly to PC and MSC, the RSC needs well-tuned cascades according to eq. (5) to (9). Next to the RSC, a linear approach of the CCC is going to be presented. As shown in Figure 7, the CCC consists similar to the PC of two position controlled drives with an additional controller within the position set point path.

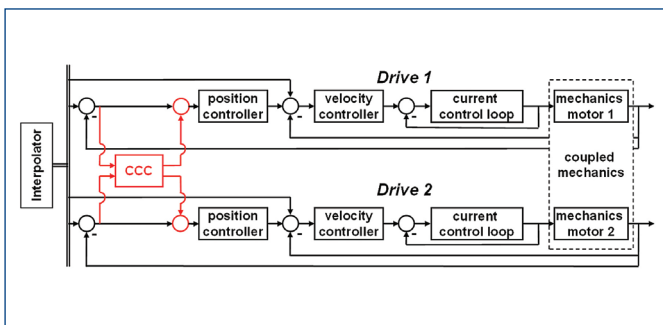


Figure 7. Structure of the Cross Coupled Control

The discussed controller has a PD-structure with the following parameters:

$$K_{PS} = 0.5 \cdot \left(\frac{D}{e_s} - 1\right) \quad (13)$$

$$K_{DS} = \frac{2\zeta \sqrt{\frac{K_p}{K_m} (1 + 2K_{PS}) - \frac{K_b}{K_m}}}{2 \frac{K_p}{K_m}} \quad (14)$$

The gain K_{PS} is going to be determined by the dynamic factor D as well as the maximum allowed position difference e_s . Depending on the system damping ζ and further parameters K_m , K_b and K_p , which are characterizing the interrelation between the motor and the mechanics, the derivation K_{DS} is going to be investigated. Beside of the additional controller the cascades are tuned corresponding to (5-9).

6. SIMULATION AND EXPERIMENTAL RESULTS

Based on the described methodology, an experimental test bench (Fig. 5, left) was created. Its mechanic and control was simulated for further comparisons of the presented control structures. The mechanics consist of the coupled drives including the two forcers with their friction and ripple forces. Both drives are linked by the elastic coupling element with stiffness and damping. Furthermore, the simulation model includes a complete servo control for each drive.

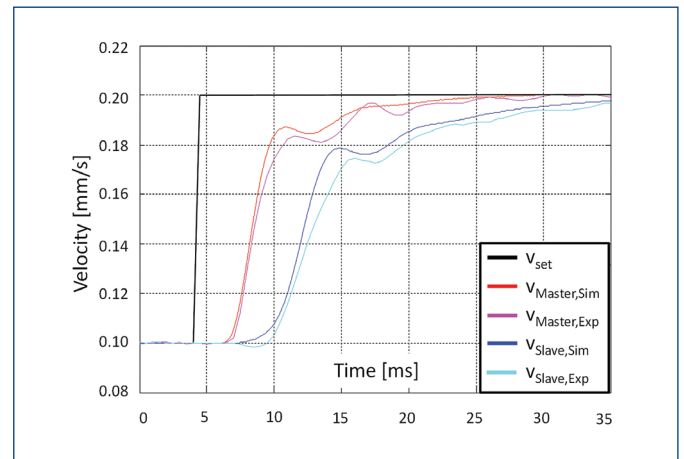


Figure 8. Comparison of the dynamic behaviour for velocity step with MSC

Fig. 8 shows the potentials of the simulation model. As can be seen, both simulation and experimental results are showing a good agreement in time domain. A validation within the frequency domain showed similar results. Therefore, further investigations have been done by using the simulation model.

For the comparison of the different control structures presented before, the frequency domain of the closed position loop was chosen. The frequency response of all of them can be seen in Fig. 9. Due to their common basis, the cascade of the servo control, they show a similar dynamic behavior.

Differences can be seen by selecting the amplitude response. Due to the additional dead times of the slave drive, MSC and RSC are showing at lower frequencies a higher damping. Compared to PC and CCC, both control structures tend to have higher peak amplitudes at higher frequencies. Within the phase response only marginal differences can be seen.

Beside the set point behavior investigations regarding to the disturbance behavior were made. Fig. 10 shows the Bode Integrals for the different control structures. Interestingly, RSC has the highest crossover frequency. This is caused by its additional synchronous controller at the fastest control loop, the current control loop. Only small differences can be

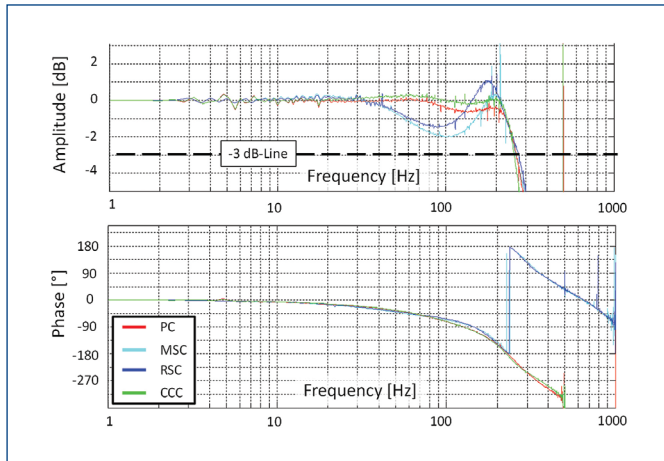


Figure 9. Frequency response of different control structures

seen comparing CCC and MSC. PC shows a slightly higher crossover frequency but also the highest amplitude. Therefore, it can be regarded as a compromise between the MSC, CCC and RSC.

7. CONCLUSION AND OUTLOOK

By using two coupled and opposite driving linear motors the reaction forces causing undesired excitation of the machine structure can be reduced. Furthermore the maximum power can be improved. The novel feed drive design was derived by the process-oriented mechatronic development methodology that offers the potentials to optimize the whole structure. Within the methodology, the controller design needs special attention due to high demands of synchronous motion. An appropriate simulation model and experimental test bench was developed. The results of the experiment and simulation showed the advantages of the drive arrangement. Regarding to the investigated control concepts, RSC showed the greatest benefits according to its disturbance behavior. Also it represents a good compromise between stability and control quality.

Future research investigations are focused on the comparison with electromechanical linear drives. Both the energy storage and the downsizing of the coupled drives are going to be further research too.

REFERENCES

- [Altintas 2011] Altintas, Y. et al. Machine tool feed drives. *CIRP Annals*, vol. 60(2), pp. 779-796, 2011. DOI: 10.1016/j.cirp.2011.05.010
- [Bruckl 1999] Bruckl, S. Feed-drive system with a permanent magnet linear motor for ultra precision machine tools. *IEEE International Conference on Power Electronics and Drive Systems*, vol. 2, pp. 821 – 826, 1999. DOI: 10.1109/PEDS.1999.792812
- [Chen 2005] Chen, C.-Y. Integrated design for a mechatronic feed drive system of machine tools. *IEEE/ASME International Conference on Advanced Intelligent Mechatronics*, pp. 588 - 593, 2005. DOI:10.1109/AIM.2006. 1511046

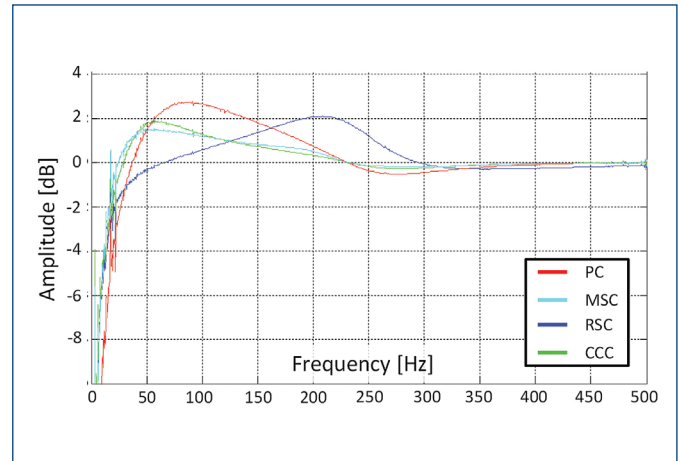


Figure 10. Comparison of the different control structures within the bode integral

[Denkena 2009] Denkena, B. et al. Energy optimized jerk-decoupling technology for translatory feed axes. *CIRP Annals*, vol. 58(1), pp. 339-342, 2009.

[Hamann 2006] Hamann, J. et al. *Elektrische Vorschubantriebe in der Automatisierungstechnik* (in German). Publicis Corporate Publishing, 2006.

[IEC 60034-1:2004] IEC 60034-1:2004(E) Rotating electrical machines – Part 30-1: Efficiency classes of line operated AC motors. International Electrotechnical Commission, 11 edition, 2004.

[Nakamura 2004] Nakamura, M. et al. *Mechatronic Servo System Control*. Springer, pp. 149-168, 2004. DOI: 10.1007/978-3-540-39921-6_7

[ODwyer 2006] O'Dwyer, A. *Handbook of PI and PID Controller Tuning Rules*, Imperial College Press, 2006.

[Rehm 2015] Rehm, M. Einordnung mechanisch gekoppelter, gegenläufig verfahrenen Direktantriebe mittels prozessorientierter Entwicklungsmethodik (in German), Thesis, Chemnitz, to be published.

[Schroeder 2001] Schroeder, D. et al. *Elektrische Antriebe – Regelung von Antriebssystemen* (in German). Springer, Berlin, 2001.

[Weidauer 2011] Weidauer, J. et al. *Elektrische Antriebstechnik*. (in German) Publicis Corporate Publishing, Erlangen, 2011.

[Zirn 2008] Zirn, O. *Machine Tool Analysis – Modeling, Simulation and Control of Machine Tool Manipulators*. Habilitation, ETH Zurich, Suisse, 2008.

CONTACTS:

Dipl. Ing. Matthias Rehm
 Technische Universität Chemnitz
 Professorship for Machine Tools and Forming Technology
 Institute for Machine Tools and Production Processes
 Chemnitz, Germany
 Straße der Nationen 62, 09111 Chemnitz, Germany
 e-mail: matthias.rehm@mb.tu-chemnitz.de
 www.tu-chemnitz.de